Magnetic Resonance in Medicine 55:316–324 (2006)

BOLD and CBV-Weighted Functional Magnetic Resonance Imaging of the Rat Somatosensory System

Shella D. Keilholz,[1] Afonso C. Silva,[2] Mira Raman,[3] Hellmut Merkle,[2] and Alan P. Koretsky[2]*

A multislice spin echo EPI sequence was used to obtain functional MR images of the entire rat brain with blood oxygenation level dependent (BOLD) and cerebral blood volume (CBV) contrast at 11.7 T. Maps of activation incidence were created by warping each image to the Paxinos rat brain atlas and marking the extent of the activated area. Incidence maps for BOLD and CBV were similar, but activation in draining veins was more prominent in the BOLD images than in the CBV images. Cerebellar activation was observed along the surface in BOLD images, but in deeper regions in the CBV images. Both effects may be explained by increased signal dropout and distortion in the EPI images after administration of the ferumoxtran-10 contrast agent for CBV fMRI. CBV-weighted incidence maps were also created for 10, 20, and 30 mg Fe/kg doses of ferumoxtran-10. The magnitude of the average percentage change during stimulation increased from 4.9% with the 10 mg Fe/kg dose to 8.7% with the 30-mg Fe/kg dose. Incidence of activation followed a similar trend. Magn Reson Med 55:316–324, 2006. Published 2005 Wiley-Liss, Inc.†

Key words: fMRI; BOLD; cerebral blood volume; somatosensory stimulation; 11.7 Tesla MRI

Rodents play an important role in neuroscience research. The development of robust whole-brain functional imaging of the rodent should have application to problems in learning, plasticity, and cortical organization. Much of the original development of functional MRI techniques was done in rodents (1–3), and many subsequent studies have examined activation in the primary sensory cortex during somatosensory stimulation (3–11). These studies have been important for understanding the basis of fMRI. Whole-brain fMRI to study an entire neural network has rarely been used in rodents even though it is routine for human fMRI. This is due in part to the need for high spatial resolution to resolve the small secondary areas in the brain. The progressive development of high-field animal scanners with strong gradients and short rise times has increased imaging speed and resolution, making high-resolution functional imaging of the whole brain feasible (12). Despite these advances, there are few studies that have examined learning or plasticity using fMRI in small animals (13,14).

There are many problems yet to be addressed in making whole-brain rodent fMRI a robust technique for neuroscience. Sensitivity is an important issue. Areas outside the primary sensory cortex (SI) may activate less strongly, and in small areas activation is further diluted by partial volume effects. In our previous work with blood oxygenation level dependent (BOLD) contrast, the incidence of activation in the thalamus, cerebellum, and secondary somatosensory cortex (SII) was 30–70% of the incidence rate in the primary somatosensory cortex (12). A functional imaging method with greater sensitivity could improve our ability to detect activation in these areas. It is also possible that the regional hemodynamic coupling is different in the secondary areas and that cerebral blood volume (CBV) or perfusion-weighted fMRI may give better results than BOLD.

CBV-weighted fMRI has been shown to increase functional contrast to noise compared to BOLD at low field strengths, which has led to its use in small animal studies and in applications of fMRI to nonhuman primates 3,15–19. As field strength increases, this advantage decreases (3). However, previous work has shown that CBV-weighted fMRI at 11.7 T can achieve activation similar to that of BOLD in the primary somatosensory cortex (20).

Several experiments have shown that BOLD and CBV-weighted fMRI have different spatial and temporal responses. Mandeville et al. determined that during a 30-s stimulation, the CBV signal is slower to reach its peak after onset and slower to return to baseline at the end of stimulation (3). Interestingly, the initial rise in CBV occurs faster than the BOLD signal (3,21). Activation seen along draining veins in the BOLD images was not apparent in the CBV-weighted images (3,21). Draining veins have long caused localization problems in BOLD fMRI, and eliminating them is particularly attractive for whole-brain imaging. However, the susceptibility gradient produced by ultrasmall superparamagnetic iron oxide (USPIO) particles injected into the blood to provide CBV weighting may cause signal dropout and image distortion, especially at high fields with fast imaging sequences such as echo planar imaging (EPI).

In this study, we compared BOLD functional imaging and CBV-weighted functional imaging for whole-brain fMRI of the rat during forepaw stimulation. Specifically, the contrast agent dose dependence for incidence of activation in different areas of the brain was studied. The presence of draining veins and the effect of image distortion were also examined.

[1]Emory University, Atlanta, Georgia, USA.
[2]National Institutes of Health, Bethesda, Maryland, USA.
[3]Stanford University, Palo Alto, California, USA.
Grant sponsor: NIH, NINDS intramural research program.
*Correspondence to: Alan P. Koretsky, Laboratory of Functional and Molecular Imaging, National Institute of Neurological Disorders and Stroke, National Institutes of Health, 10 Center Drive, 10/B1D728, MSC 1065, Bethesda, MD 20892, USA. E-mail: KoretskyA@ninds.nih.gov
Received 8 March 2005; revised 24 August 2005; accepted 31 August 2005.
DOI 10.1002/mrm.20744
Published online 21 December 2005 in Wiley InterScience (www.interscience.wiley.com).

METHODS

Animal Preparation

All experiments were performed in compliance with guidelines set by the National Institutes of Neurologic Disorders and Stroke ACUC. Twenty-four adult male Sprague–Dawley rats (150–311 g) were initially anesthetized with 5% halothane and maintained at 1.5% halothane during the following surgical procedures. Each rat was orally intubated and placed on a mechanical ventilator throughout the surgery and the experiment. Polyethylene catheters were inserted into the right femoral artery and vein to allow monitoring of arterial blood gases and administration of drugs. Two needle electrodes were inserted just under the skin of each forepaw, one between digits 1 and 2 and the other between digits 3 and 4. After surgery, the rat was given an i.v. bolus of α-chloralose (80 mg/kg) and halothane was discontinued. Anesthesia was maintained with a constant α-chloralose infusion (27 mg/kg/hr) (9).

The rat was placed on a heated water pad to maintain rectal temperature at approximately 37°C while in the magnet. Each animal was secured in a head holder with ear bars and a bite bar to prevent head motion and was strapped to a plastic cradle. End-tidal CO_2, rectal temperature, tidal pressure of ventilation, heart rate, and arterial blood pressure were continuously monitored during the experiment. Arterial blood gas levels were checked periodically and corrections were made by adjusting respiratory volume or administering sodium bicarbonate to maintain normal levels when required. An i.v. injection of pancuronium bromide (4 mg/kg) was given once per hour to prevent motion. After BOLD fMRI studies were finished, the rats were i.v.: either given 10 mg Fe/kg (6 rats), 20 mg Fe/kg (10 rats), or 30 mg Fe/kg (10 rats) of ferumoxtran-10, a dextran-coated superparamagnetic iron oxide particle with a long blood half-life (Combidex, AMI-227, gift of Advanced Magnetics, Inc., Cambridge, MA, USA). Two rats were given 10 mg Fe/kg followed by 20 mg Fe/kg and are included in both the 10- and the 30-mg groups.

MRI

All images were acquired with an 11.7 T/31 cm horizontal bore magnet (Magnex, Abingdon, UK), interfaced to an AVANCE console (Bruker, Billerica, MA, USA) and equipped with a 9-cm gradient set, capable of providing 45 G/cm with a rise time of 75 μs. Shimming was performed with a custom-built shim set and high power shim supply (Resonance Research Inc; Billerica, MA, USA). Excitation was provided by a homebuilt 70-mm inner diameter birdcage coil. A contoured rectangular surface coil (2 × 3 cm) that attached to the head holder was used to receive the MR signal. Scout images were acquired in three planes with a fast spin echo sequence to determine appropriate positioning for the functional study.

A spin echo EPI sequence was used for the fMRI studies. Setup included shimming, adjustments to echo spacing and symmetry, and B_0 compensation. For BOLD fMRI studies, a single-shot sequence with a 64 × 64 matrix was run with the following parameters: effective echo time 30 ms, repetition time 1.5 s, bandwidth 200 kHz, field of view 1.92 × 1.92 cm. Whole-brain coverage was obtained with ten to eleven 2-mm-thick slices, spaced 0.2 mm apart. For the CBV-weighted studies, the bandwidth was increased to 250 kHz, allowing the effective echo time to be shortened to 20 ms.

Anatomic images were also obtained from one rat to depict the surface vasculature of the rat brain, which may contribute to the BOLD signal. A 3D FLASH sequence with the following parameters was used: TE 5 ms, TR 20 ms, flip angle (FA) 15°, matrix size 384 × 192 × 256. This gave an isotropic resolution of 100 μm.

Somatosensory Stimulation Paradigm

A World Precision Instruments stimulator (WPI, Sarasota, FL, USA) supplied 2-mA, 300-μs pulses repeated at 3 Hz to both forepaws upon demand. The paradigm consisted of 10 dummy scans to reach steady state, followed by 60 scans during rest, 30 scans during forepaw stimulation, and a final 60 scans during rest, for a total experiment time of 4 min. The animal was allowed to rest for approximately 3 to 5 min, and then the stimulation paradigm was repeated.

Data Analysis

Analysis of the time series was performed using STIMULATE (University of Minnesota). A correlation coefficient was calculated from cross-correlation of the unfiltered time series with a boxcar waveform representing the stimulation period. The activation threshold was set at 0.2, and only groups that included at least four activated pixels were considered significant. One to three fMRI series from each animal were analyzed, depending on the physiologic stability of the animal. Time courses from activated pixels in SI, SII, thalamus, and cerebellum were recorded and averaged to form a representative response for each region. A linear baseline correction was performed on all time courses.

Using a customized program developed in-house, the Paxinos rat brain atlas (22) was digitized so it could be warped to each MRI slice containing a specific region of interest. The location of the activated pixels of that slice in relation to the atlas could be saved. The same program was then used to read in the atlas images with activated pixels from each rat and add them together to display the relative incidence of activation in each region in the atlas coordinate system.

For the dose-dependent CBV-weighted studies, the incidence of activation in each area for each dose was recorded. Time courses were measured for a 3 × 3 pixel area in SI for each dose.

RESULTS

Excellent echo-planar images were obtained both before and after the injection of the ferumoxtran-10. Images obtained with parameters used for BOLD fMRI and CBV-weighted images acquired after injection of 20 mg Fe/kg are shown in Fig. 1. The contrast agent reduced the overall signal, but this effect was partially offset by shortening the effective echo time to 20 ms. Compared to the BOLD image

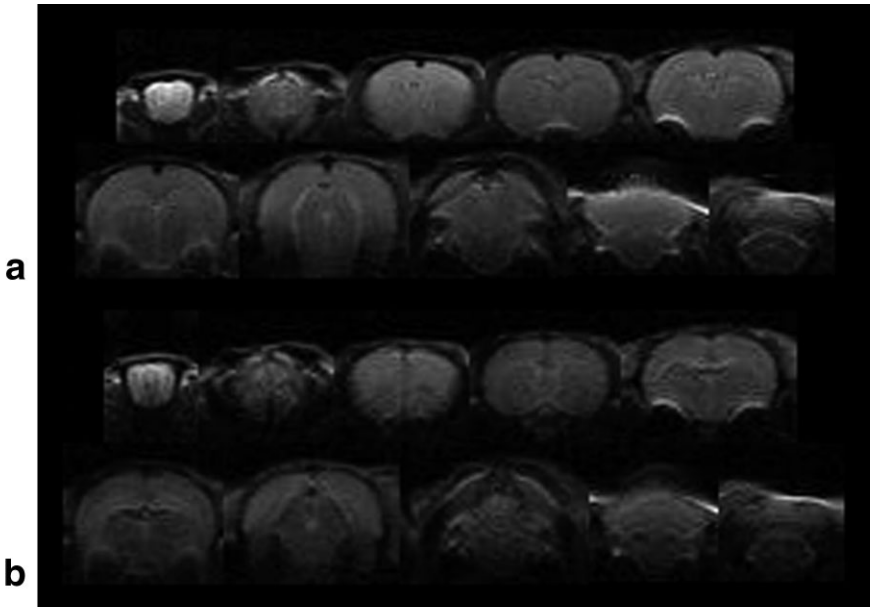

FIG. 1. (**a**) Ten EPI images covering the whole rat brain, acquired with the parameters used for BOLD experiments. (**b**) EPI images of the same rat after the administration of 20 mg Fe/kg ferumoxtran-10, acquired with the parameters used for CBV experiments. Blood vessels appear dark and the contrast between gray and white matter is reversed.

(with 30 ms TE), signal intensity after ferumoxtran-10 administration was 24% greater for 10 mg Fe/kg, 0.7% greater for 20 mg Fe/kg, and 32% lower for 30 mg Fe/kg. Blood vessels appear dark after administration of the contrast agent, and signal losses are particularly evident in large vessels near the surface of the brain. Figure 2 shows images from before and after ferumoxtran-10 injection fit to the Paxinos atlas. Differences are quite apparent. Measurements made along the midline of the brain, where the greatest signal dropout on the surface near SI occurs, show a 4.6% shortening of the apparent MRI length of the brain for the 10 mg Fe/kg dose compared to EPI images without ferumoxtran-10, a 14.7% shortening for the 20 mg Fe/kg dose, and a 20.2% shortening for the 30 mg Fe/kg dose. Measurements made of the gap between the visual cortex and colliculus in the precerebellar slice, where the largest signal dropout occurs, show a 62% gap increase after injection of 10 mg Fe/kg, an 88% increase after 20 mg Fe/kg, and a 111% increase after 30 mg Fe/kg.

Activation in SI during electrical stimulation of the forepaw was observed with both BOLD and CBV-weighted fMRI in all rats. Typical activation maps are shown in Fig. 3. In the CBV-weighted images, the extent of activation increases with increasing ferumoxtran-10 doses. A line of activated pixels extending from SI to the sagittal sinus that appears to indicate a draining vein was often observed in the BOLD images, but was seen much less frequently in the CBV-weighted images.

Average time courses from SI for BOLD and CBV-weighted fMRI are shown in Fig. 4. Rats injected with 10 mg Fe/kg ferumoxtran-10 showed the lowest average percentage change in SI during stimulation (4.9 ± 2.3%). The 20 mg Fe/kg dose gave a change of 5.9 ± 1.8%, and the 30 mg Fe/kg dose caused an 8.7 ± 2.4% change during

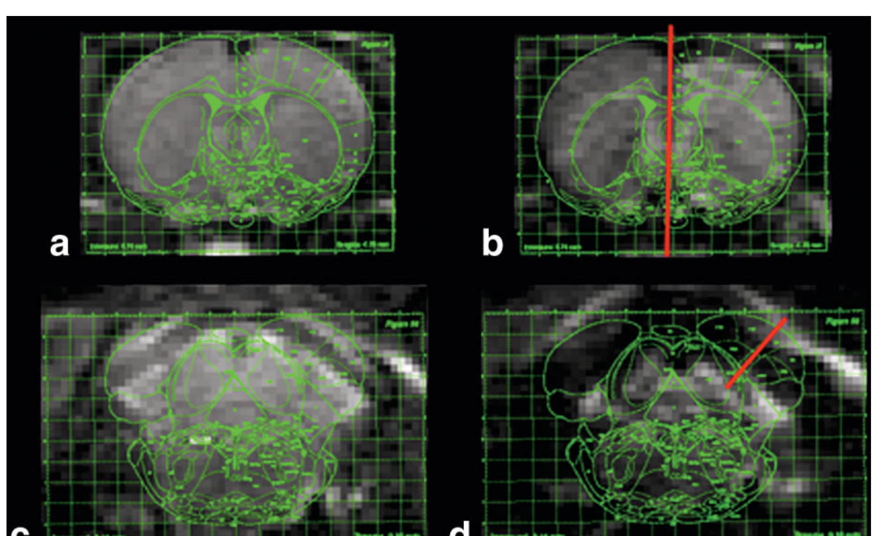

FIG. 2. Two image slices from the same rat before and after administration of 30 mg Fe/kg ferumoxtran-10, fitted to the Paxinos atlas using the same warp. (**a**) The slice containing SI before and after (**b**) ferumoxtran-10 administration. Signal from the surface is lost. (**c**) The precerebellar slice before and after (**d**) ferumoxtran-10 administration. Large signal shifts are evident. Red lines indicate profile measurements.

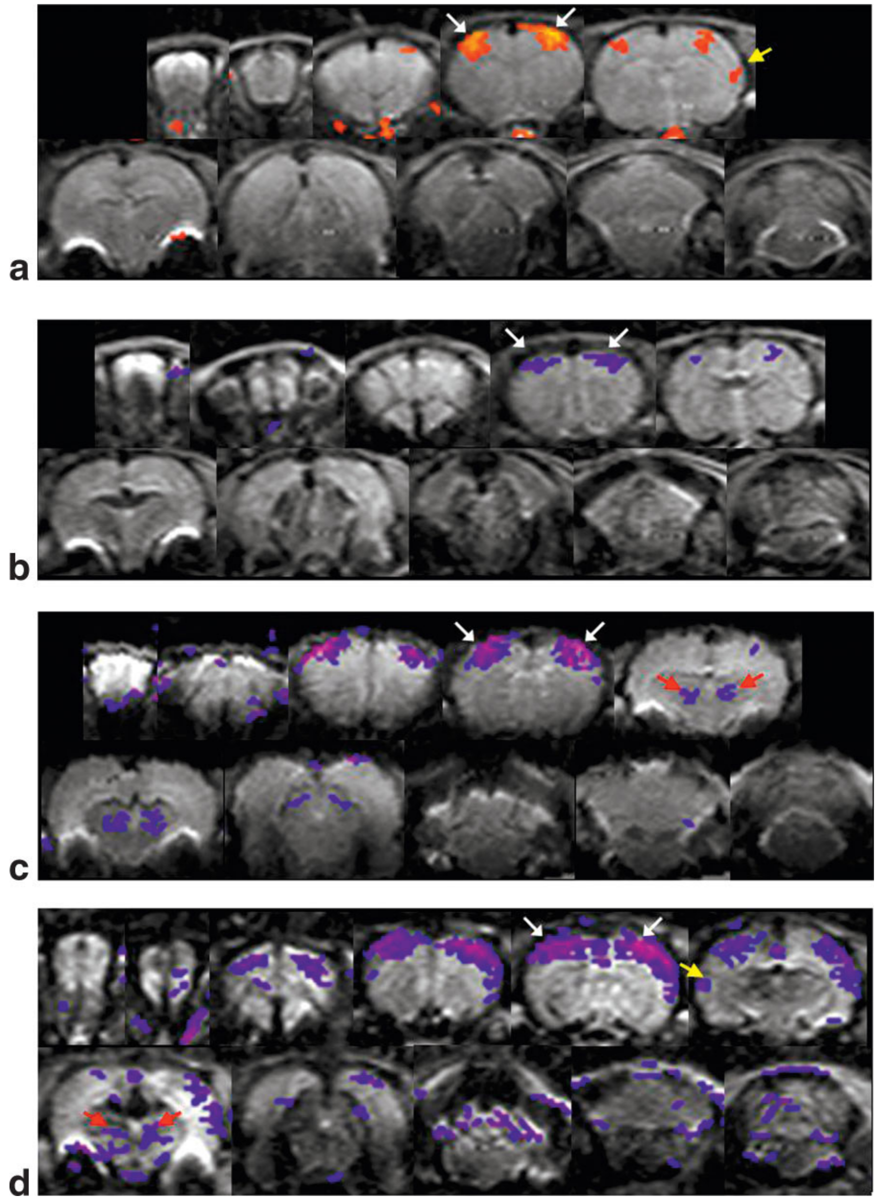

FIG. 3. (**a**) Typical BOLD functional images acquired during electrical stimulation of the forepaw, showing activation in SI (white arrows) and SII (yellow arrow). (**b–d**) Typical CBV functional images of forepaw stimulation with 10 (b), 20 (c), and 30 mg Fe/kg (d) ferumoxtran-10, showing activation in SI (white arrows), SII (yellow arrow), and the thalamus (red arrows).

activation. Signal fluctuations in the baseline images were similar for all doses, having a SD of 1.3% for the 10 mg Fe/kg dose, 1.0% for the 20 mg Fe/kg dose, and 1.2% for the 30 mg Fe/kg dose. Rats showed no adverse reaction to the higher contrast dose.

A poststimulus undershoot of approximately 1% (significantly different from baseline signal; $P < 0.01$) was observed in the BOLD time course. This undershoot begins shortly after the end of stimulation and persists for approximately 30 s. No overshoot was seen in the CBV-weighted time courses, but the signal took approximately 30 s to return to baseline.

SII showed average changes of 3.0 ± 2.1% for BOLD fMRI, 3.3 ± 2.3% for 20 mg Fe/kg CBV-weighted fMRI, and 5.1 ± 3.0% for 30 mg Fe/kg CBV-weighted fMRI. No average change was calculated for secondary areas for the 10 mg Fe/kg dose due to the low incidence of detectable activation. Changes of approximately 3.3 ± 3.4% were also observed in the cerebellum with BOLD fMRI and 4.0 ± 2.2% with 20 mg Fe/kg CBV-weighted fMRI. A change of 3.9 ± 1.9% was observed with 30 mg Fe/kg CBV-weighted fMRI. The thalamus had the smallest change during activation (approximately 2.6 ± 1.6% for BOLD fMRI, 3.0 ± 1.7% for 20 mg Fe/kg CBV-weighted fMRI, and 3.7 ± 2.3% for 30 mg Fe/kg CBV-weighted fMRI).

Incidence maps of BOLD and CBV-weighted fMRI scans are shown in Fig. 5. Similar incidence of activation was observed with the two methods. With BOLD and CBV-weighted fMRI at 20 mg Fe/kg of ferumoxtran-10, activation is observed in SI in all the scans, in SII in 50–60% of the scans, in the cerebellum in 60–70% of the scans, and in the thalamus in 20–30% of the scans. CBV-weighted fMRI at 30 mg Fe/kg had similar incidence but thalamic activation was observed in 50% of the scans. Little activation outside of SI was detected with the 10 mg Fe/kg CBV-weighted fMRI. These results are summarized in Tables 1 and 2.

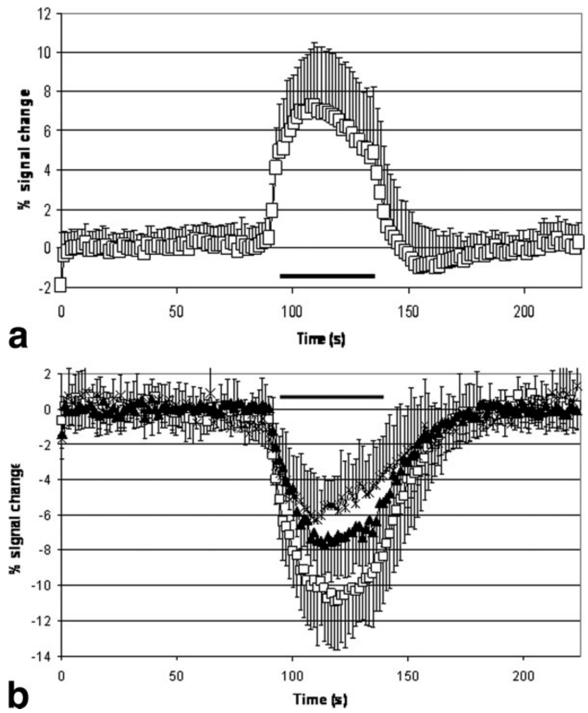

FIG. 4. Average time courses from SI measured with BOLD (**a**) or CBV (**b**) fMRI. In b, averages for three ferumoxtran-10 doses are shown: stars, 10 mg Fe/kg; triangles, 20 mg Fe/kg; and squares, 30 mg Fe/kg. The black bar indicates the stimulation period.

Draining veins on the surface of SI running toward the sagittal sinus in the BOLD images were readily apparent in the incidence maps. These veins are less pronounced in the CBV-weighted maps. The other major difference between the BOLD fMRI and CBV-weighted fMRI was the pattern of cerebellar activation. In the BOLD images, most cerebellar activation occurs near the surface, and bilateral focal areas are visible. In the CBV-weighted images, very little activation occurs near the surface. There is also a shift in activation seen in the CBV-weighted fMRI compared to the BOLD fMRI in the slice anterior to the cerebellum.

Anatomic images obtained with a FLASH sequence from one rat clearly depict large vessels on the surface of the cortex and cerebellum (Fig. 6). The vessels in the cerebellum correspond roughly to the bilateral focal areas of activation detected in the BOLD fMRI incidence maps. Finally, to verify that the veins detected on the surface of SI were due to BOLD-based signal changes and not due to inflow activation, maps of a single slice were made at 1.5 s repetition time and at 10 s repetition time. Figure 7 shows that the presence of the draining vein was not affected by the repetition time, indicating it was due to BOLD effects rather than inflow effects.

DISCUSSION

BOLD and CBV-weighted fMRI demonstrated similar sensitivity to activation in multiple areas of the somatosensory system during electrical stimulation of the forepaw. Although the overall rates of incidence are similar, not all animals showed activation in the same areas with BOLD

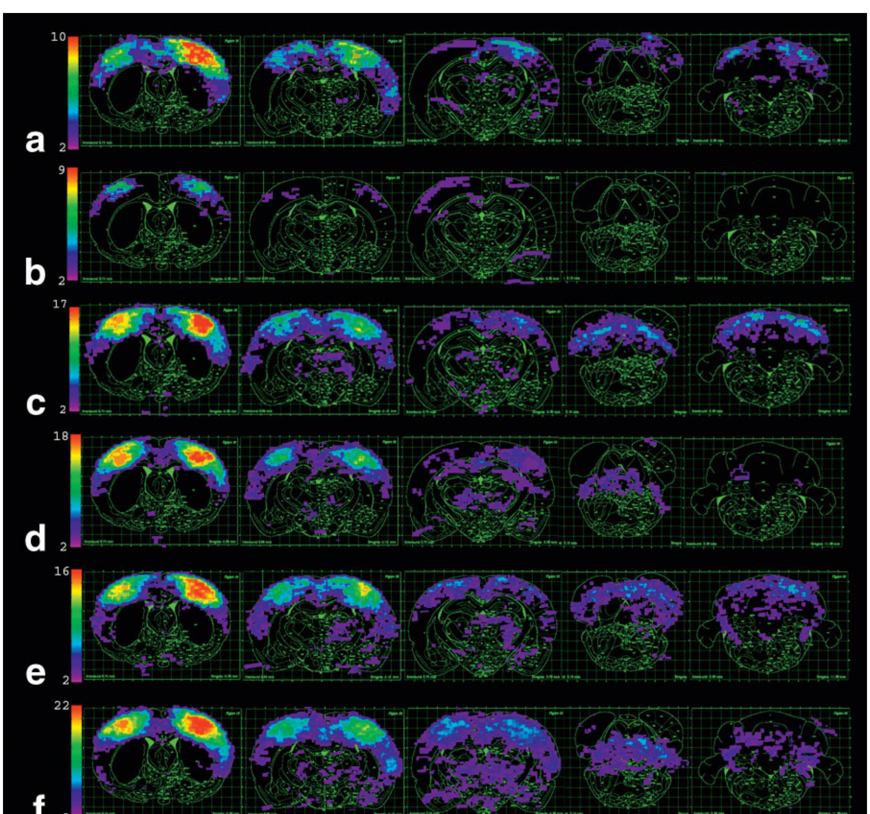

FIG. 5. Incidence maps for slices containing SI, SII, thalamus, and cerebellum. Incidence ranges from 2 to 10 animals. BOLD maps (**a**, **c**, **e**) from the same animals are shown with CBV maps at 10 (**b**), 20 (**d**), and 30 mg Fe/kg (**f**) of ferumoxtran-10. Draining veins are prominent in the BOLD maps but less pronounced in the CBV maps, and cerebellar activation is shifted away from the surface in the CBV maps.

Table 1
Summary of Incidence for BOLD and CBV Scans.

	BOLD rats	BOLD scans	10 mg/kg CBV rats	10 mg/kg CBV scans	20 mg/kg CBV rats	20 mg/kg CBV scans	30 mg/kg CBV rats	30 mg/kg CBV scans
SI	24/24	43/43	6/6	9/9	10/10	20/20	10/10	21/21
SII	13/24	20/43	1/6	1/9	5/10	9/20	7/10	13/21
Thalamus	7/24	9/43	0/6	0/9	2/10	3/20	8/10	10/21
Cerebellum	18/24	29/43	0/6	0/9	7/10	11/20	6/10	11/21

and CBV-weighted fMRI. For example, in some animals SII would show activation in CBV-weighted maps but not in BOLD maps, or vice versa. This is probably due to the fact that areas outside of SI showed lower incidences of activation than SI and therefore it was sometimes the case that an area activated during BOLD detection but not CBV detection. We previously suggested that partial volume effects could account in part for the variation in the number of areas that activate from rat to rat (12). However, since the imaging geometry was identical for both CBV-weighted and BOLD fMRI, the differences in incidence of activation seen between the two techniques cannot be attributed to partial volume effects alone, and regional hemodynamics may contribute to the variation. Another factor is that CBV-weighted and BOLD fMRI have different dependences upon resting blood volume, which could influence their sensitivities to activation in different areas (15).

The amount of change during stimulation observed with CBV-weighted fMRI in this study was reasonable compared to that previously reported. Van Bruggen et al. and Palmer et al. measured average signal changes of 9 and 13.5%, respectively, with gradient echo sequences at 4.7 T, a contrast dose of 6 mg/kg, and a TE of 12–17 ms (17,18). The differences in our imaging parameters and the use of spin echo rather than gradient echo EPI do not permit a direct comparison, but the average 8% signal change we measured during stimulation is within the range expected.

Table 2.
Incidence and Dose-Dependence for USPIO Compared with BOLD in the Same Rats.

	10 mg/kg CBV	BOLD
SI	6/6	6/6
SII	1/6	4/6
Thalamus	0/6	2/6
Cerebellum	0/6	3/6
	20 mg/kg CBV	**BOLD**
SI	10/10	10/10
SII	5/10	7/10
Thalamus	2/10	2/10
Cerebellum	7/10	8/10
	30 mg/kg CBV	**BOLD**
SI	10/10	10/10
SII	7/10	6/10
Thalamus	8/10	3/10
Cerebellum	6/10	7/10

While we did not attempt to quantify the change in CBV during stimulation in this experiment, a rough estimate can be made using a T_2 value for the rat cortex at 11.7 T of 38 ms measured previously (unpublished). Following Mandeville's method, the percentage change during stimulation then corresponds to an absolute CBV change of approximately 23% for the 20 mg Fe/kg dose, similar to the 24% reported by Mandeville et al. (3). Using the same T_2 to calculate the drop in signal intensity after ferumoxtran-10 administration gives a signal loss of 7% for the 10 mg Fe/kg dose, 32% for the 20 mg Fe/kg dose, and 62% for the 30 mg Fe/kg dose. As the optimal dose for a given TE should reduce signal by about 60%, the 30 mg Fe/kg dose should provide the maximum contrast to noise for these parameters. We expect no observable contribution of the BOLD effect to the CBV-weighted signal change because of the extremely short T_2^* of blood at this field strength with ferumoxtran-10. The T_2^* of arterial blood was measured at 0.85 ms after the rat was injected with 11 mg Fe/kg (23).

One of the major differences between the functional images obtained with BOLD and CBV-weighted fMRI is the prominence of draining veins in the BOLD fMRI maps. The relative contributions of vessels of different sizes have been a long-standing issue in BOLD fMRI (6,24,25). The BOLD signal comes from both large and small vessels, and each vessel can contribute from both intravascular and extravascular compartments. The extravascular signal from small vessels is generally considered the most localized to neuronal activity, but it can easily be overwhelmed by large signal from inside vessels and around large draining veins. Spin-echo imaging as used in the present work is expected to reduce the signal from around large draining veins compared to gradient echo imaging, because of the refocusing effect of the 180° pulse (24,25). Simulations and experiments have argued that the intravascular contribution to spin-echo BOLD imaging is small at high fields, due to the short T_2 and T_2^* of venous blood (6). Nevertheless, activation along what appear to be draining veins, stretching from SI across the cerebral surface to the sagittal sinus, have been observed both in this study and in previous work at 11.7 T (10,12). This activation is not due to inflow effects, as it was unaffected when the repetition time was increased from 1.5 to 10 s (Fig. 7). The signal may arise from incomplete suppression of the extravascular spins surrounding large vessels or from residual intravascular signal. Although we used a spin-echo EPI sequence, there is significant T_2^* weighting during the readout, which can contribute to the BOLD fMRI map.

In contrast to the BOLD fMRI, few distinct draining veins were observed with the CBV-weighted fMRI. Similar

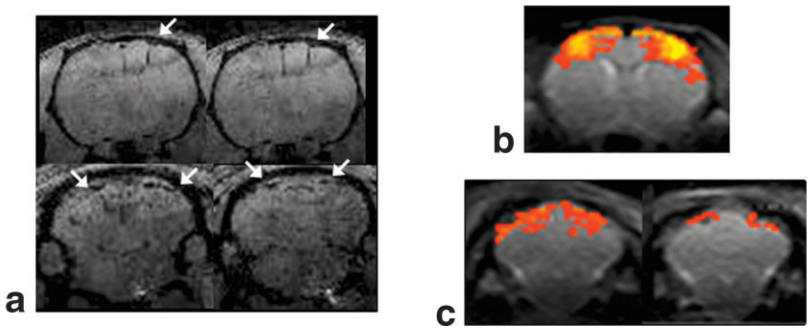

FIG. 6. (**a**) Anatomic images of the primary sensory cortex and cerebellum acquired with 100-μm isotropic resolution. White arrows indicate blood vessels. (**b**) A BOLD functional map of the primary somatosensory cortex. A line of activation runs along the surface of the brain from SI toward the sagittal sinus, corresponding to the vessel seen in the anatomic image. (**c**) BOLD functional maps from two rats, showing bilateral foci of activation near the surface of the cerebellum. These correspond to the surface vessels seen in the anatomic image.

results were reported by Mandeville and Marota (15). The lack of draining veins has been attributed to the small volume change in large vessels and to the T_2^*-shortening effect of the contrast agent. However, a careful comparison of the MRI slice from the SI region of the brain before and after ferumoxtran-10 administration (Fig. 2) shows significant signal loss around the surface of the brain, particularly near the top. If the T_2* in these areas is short enough to cause signal dropout, distortion is likely to be present as well with the long acquisition times used in this study. Thus, activation from the draining veins may be lost or shifted deeper into the cortex due to the large susceptibility effect of the contrast agent. In some of the CBV-weighted incidence maps (for example, the second slice in Fig. 5d and f), there appears to be activation from draining veins that is shifted away from the surface by the susceptibility effect of the contrast agent in the sagittal sinus.

The other key difference noted in this study was the location of cerebellar activation in the BOLD and CBV-weighted fMRI activation maps. In the slice containing most of the cerebellum (the last slice in Fig. 5), the activation in the CBV-weighted incidence maps is shifted downward by 1–2 mm with respect to the activation in the BOLD incidence map of the same slice. Also, the slice anterior to the main cerebellar slice, which contains cerebellum, pons, colliculus, etc., often shows activation near the center of the image in the CBV-weighted map, but the only activation is along the surface in the BOLD map. A similar disparity between BOLD and CBV-weighted activation maps was reported in a recent study by Mandeville et al. using cocaine administration (19).

There are several hypotheses that can be made about this shift. One is that the shift is due to the different vascular weightings of the BOLD and CBV-weighted techniques. Mandeville and Marota found that activation in SI with CBV-weighted fMRI was shifted medially (0.26 mm) and dorsally (0.45–0.67 mm) compared to the activation seen with BOLD fMRI (15). When the vascular weighting was taken into account, the activation colocalized. While the measurement and correction of vascular weighting was beyond the scope of this study, it is a direction for future work.

Another hypothesis is that the BOLD activation is heavily weighted toward draining veins and the CBV-weighted fMRI depicts the true activated area. The observed draining veins near SI in the BOLD images demonstrate that this is a possibility, and anatomic images show surface vessels near the bilateral focal points of activation (Fig. 6). Much of the activation in the slice anterior to the cerebellum was near the sagittal sinus. Recently high-resolution fMRI studies of rat, cat, and human sensory cortex indicate that the largest contribution to BOLD fMRI using gradient echo sequences is from surface vessels (6,10,26,27). It is interesting that even with spin-echo weighting at 11.7 T, high BOLD fMRI activation is still observed from surface vessels.

The most probable possibility is that the susceptibility differences created by the injection of the contrast agent cause signal dropout and image distortion, moving the apparent source of activation. The shortening of T_2 and T_2^* upon administration of contrast agent causes the signal at a given TE to decrease (drop out). Upon careful examination, it is apparent that signal voids appear after the administration of the contrast agent, mostly near the surfaces of the brain (Fig. 2). We attempted to alleviate this by using the shortest TE possible for our imaging parameters. In-

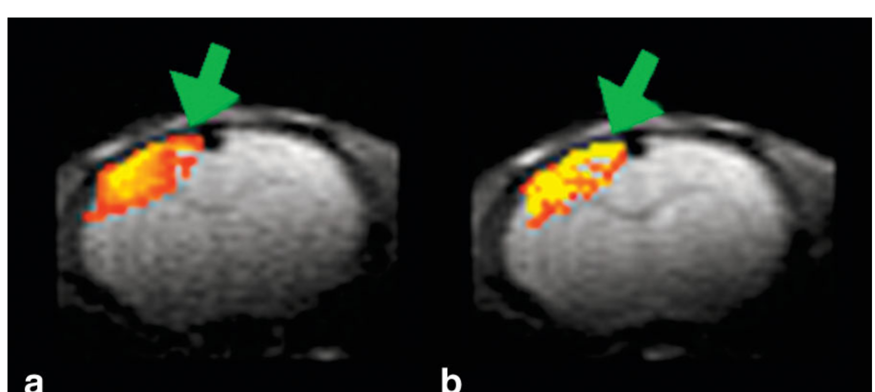

FIG. 7. (**a**) A functional map of a single slice acquired during stimulation of one forepaw with the usual paradigm of 60 rest images, 30 active images, and 60 rest images, with a TR of 1.5 s. Activation in the draining vein is clearly visible (arrow). Correlation coefficients range from 0.2 to 0.8. (**b**) A functional map from the same animal with a TR of 10 s and a paradigm of 10 rest images, 5 active images, and 10 rest images. Activation in the draining vein is apparent (arrow). Correlation coefficients range from 0.5 to 0.8.

deed, the SNR of the post-ferumoxtran-10 images at TE = 20 ms was better than the SNR of the preinjection BOLD images at TE = 30 ms. However, the reduced relaxation times after ferumoxtran-10 administration also cause geometric distortions, due to the long acquisition time of the EPI sequence. In order to keep our spatial resolution between BOLD and CBV-weighted images the same, we did not decrease the acquisition time for the CBV-weighted experiments. Therefore, significant distortions should be present, especially in the slice anterior to the cerebellum, where the signal appears to be shifted both upward and downward from the vascular region near the center of the image. Other problematic areas include the olfactory bulbs and along the cortical surface (compare Figs. 1b and 2b, after contrast injection, with Figs. 1a and 2a, respectively, before contrast injection). These distortions could account for much of the dislocation between the BOLD and CBV-weighted maps. Nevertheless, vascular weighting and sensitivity to draining veins may contribute as well. Without sacrificing spatial resolution, it may be necessary to shorten the EPI acquisition time, either by using stronger gradients or by resorting to parallel imaging techniques, in order to minimize the distortion effects. However, at typically used parameters, it is clear that the doses of ferumoxtran-10 used can significantly affect the images.

There has been much interest in comparing the detailed localization and extent of activation detected by BOLD compared to perfusion or CBV-based fMRI techniques in both humans and SI cortex in animals (28–30). These comparisons have been made over the entire extent of activation as well as the subcortical extent of activation, for example, in ocular dominance columns (31). In almost all of these cases, significant differences were detected, with either the perfusion or the CBV-based fMRI appearing to localize better. There is no quantitative explanation for this but all of the factors that might affect the present results, such as differential sensitivity to draining veins, differential effects on image distortion, and differences in neurovascular coupling, could be responsible.

The dose-dependent studies in this experiment indicated that 10 mg Fe/kg ferumoxtran-10, commonly used at lower field strengths, is insufficient to detect activation in secondary areas with spin-echo EPI at 11.7 T. A dose of 20 mg Fe/kg gives an incidence of activation similar to BOLD. While a larger change was observed in SI with 30 mg Fe/kg ferumoxtran-10, the high contrast dose leads to greater signal dropout. It may also increase the incidence of observable activation in the thalamus, but more studies must be performed to determine whether this effect is significant.

In general, CBV-weighted fMRI demonstrates sensitivity to activation outside of SI similar to that of BOLD, but with apparently less contamination from large vessels. However, the signal dropout caused by the ferumoxtran-10 particles may explain the apparent loss of large vessel contamination and makes CBV-weighted fMRI a poor choice for imaging certain regions, like the cerebellum where signal droupout significantly distorts the image. Developing strategies to minimize the signal dropout encountered with CBV-weighted fMRI will be important for robust application of rodent whole-brain CBV-weighted fMRI to the study of learning and plasticity. BOLD has the advantage in that no exogenous contrast agent is needed, and the incidence maps generated are of similar quality to the maps generated with ferumoxtran-10. The disadvantage of BOLD continues to be the presence of draining veins that might cause mislocalization even in the rat brain using spin-echo EPI at 11.7 T.

ACKNOWLEDGMENTS

The authors thank Torri Wilson for animal preparation and physiology and Piotr Starewicz of Resonance Research, Inc., for the custom-built shim set.

REFERENCES

1. Williams DS, Detre JA, Leigh JS, Koretsky AP. Magnetic resonance imaging of perfusion using spin inversion of arterial water. Proc Natl Acad Sci USA 1992;89:212–216.
2. Ogawa S, Lee TM, Kay AR, Tank DW. Brain magnetic resonance imaging with contrast dependent on blood oxygenation. Proc Natl Acad Sci USA 1990;87:9868–9872.
3. Mandeville JB, Marota JJ, Kosofsky BE, Keltner JR, Weissleder R, Rosen BR, Weisskoff RM. Dynamic functional imaging of relative cerebral blood volume during rat forepaw stimulation. Magn Reson Med 1998; 39:615–624.
4. Bock C, Krep H, Brinker G, Hoehn-Berlage M. Brainmapping of alpha-chloralose anesthetized rats with $T2^*$-weighted imaging: distinction between the representation of the forepaw and hindpaw in the somatosensory cortex. NMR Biomed 1998;11:115–119.
5. Hyder F, Behar KL, Martin MA, Blamire AM, Shulman RG. Dynamic magnetic resonance imaging of the rat brain during forepaw stimulation. J Cereb Blood Flow Metab 1994;14:649–655.
6. Lee SP, Silva AC, Ugurbil K, Kim SG. Diffusion-weighted spin-echo fMRI at 9.4 T: microvascular/tissue contribution to BOLD signal changes. Magn Reson Med 1999;42:919–928.
7. Marota JJ, Ayata C, Moskowitz MA, Weisskoff RM, Rosen BR, Mandeville JB. Investigation of the early response to rat forepaw stimulation. Magn Reson Med 1999;41:247–252.
8. Ogawa S, Lee TM, Stepnoski R, Chen W, Zhu XH, Ugurbil K. An approach to probe some neural systems interaction by functional MRI at neural time scale down to milliseconds. Proc Natl Acad Sci USA 2000;97:11026–11031.
9. Silva AC, Lee SP, Yang G, Iadecola C, Kim SG. Simultaneous blood oxygenation level-dependent and cerebral blood flow functional magnetic resonance imaging during forepaw stimulation in the rat. J Cereb Blood Flow Metab 1999;19:871–879.
10. Silva AC, Koretsky AP. Laminar specificity of functional MRI onset times during somatosensory stimulation in rat. Proc Natl Acad Sci USA 2002;99:15182–15187.
11. Spenger C, Josephson A, Klason T, Hoehn-Berlage M, Schwindt M, Ingvar M, Olson L. Functional MRI at 4.7 tesla of the rat brain during electric stimulation of forepaw, hindpaw, or tail in single- and multislice experiments. Exp Neurol 2000;166:246–253.
12. Keilholz SD, Silva AC, Raman M, Merkle H, Koretsky AP. Functional MRI of the rodent somatosensory pathway using multislice echo planar imaging. Magn Reson Med 2004;52:89–99.
13. Dijkhuizen RM, Ren JM, Mandeville JB, Wu O, Ozdag FM, Moskowitz MA, Rosen BR, Finklestein SP. Functional magnetic resonance imaging of reorganization in rat brain after stroke. Proc Natl Acad Sci USA 2001;98:12766–12771.
14. Miller MJ, Chen N, Limin L, Tom B, Weiss C, Disterhoft JF, Wyrwicz AM. fMRI of the conscious rabbit during unilateral classical eyeblink conditioning reveals bilateral cerebellar activation. J Neurosci 2003;23: 11753–11758.
15. Mandeville JB, Marota JJ. Vascular filters of functional MRI: spatial localization using BOLD and CBV contrast. Magn Reson Med 1999;42: 591–598.
16. Mandeville JB, Jenkins BG, Kosofsky BE, Moskowitz MA, Rosen BR, Marota JJ. Regional sensitivity and coupling of BOLD and CBV changes during stimulation of rat brain. Magn Reson Med 2001;45:443–447.

17. Palmer JT, de Crespigny AJ, Williams S, Busch E, van Bruggen N. High-resolution mapping of discrete representational areas in rat somatosensory cortex using blood volume-dependent functional MRI. Neuroimage 1999;9:383–392.
18. van Bruggen N, Busch E, Palmer JT, Williams SP, de Crespigny AJ. High-resolution functional magnetic resonance imaging of the rat brain: mapping changes in cerebral blood volume using iron oxide contrast media. J Cereb Blood Flow Metab 1998;18:1178–1183.
19. Mandeville JB, Jenkins BG, Chen YC, Choi JK, Kim YR, Belen D, Liu C, Kosofsky BE, Marota JJ. Exogenous contrast agent improves sensitivity of gradient-echo functional magnetic resonance imaging at 9.4 T. Magn Reson Med 2004;52:1272–1281.
20. Silva AC, Koretsky AP, Kellman P, Duyn JH. fMRI impulse response for BOLD and CBV contrast in rat somatosensory cortex. In: Proceedings of the 12th Annual Meeting of ISMRM, Kyoto, Japan, 2004. p 277.
21. Leite FP, Tsao D, Vanduffel W, Fize D, Sasaki Y, Wald LL, Dale AM, Kwong KK, Orban GA, Rosen BR, Tootell RB, Mandeville JB. Repeated fMRI using iron oxide contrast agent in awake, behaving macaques at 3 Tesla. Neuroimage 2002;16:283–294.
22. Paxinos G, Watson C. The rat brain in stereotaxic coordinates. San Diego: Academic Press, 1998.
23. Barbier EL, St Lawrence KS, Grillon E, Koretsky AP, Decorps M. A model of blood-brain barrier permeability to water: accounting for blood inflow and longitudinal relaxation effects. Magn Reson Med 2002;47:1100–1109.
24. Ogawa S, Menon RS, Tank DW, Kim S-G, Merkle H, Ellermann JM, Ugurbil K. Functional brain mapping by blood oxygenation level-dependent contrast magnetic resonance imaging. A comparison of signal characteristics with a biophysical model. Biophys J 1993;64: 803–812.
25. Weisskoff RM, Zuo CS, Boxerman JL, Rosen BR. Microscopic susceptibility variation and transverse relaxation: theory and experiment. Magn Reson Med 1994;31:601–610.
26. Zhao F, Wang P, Kim S-G. Cortical depth-dependent gradient-echo and spin-echoBOLD fMRI at 9.4T. Magn Reson Med 2004;51:518–524.
27. Pfeuffer J, Adriany G, Shmuel A, Yacoub E, Van De Moortele, P-F, Hu X, Ugurbil K. Perfusion-based high-resolution functional imaging in the human brain at 7 tesla. Magn Reson Med 2002;47:903–911.
28. Luh WM, Wong EC, Bandettini PA, Ward BD, Hyde JS. Comparison of simultaneously measured perfusion and BOLD signal increases during brain activation with T(1)-based tissue identification. Magn Reson Med 2000;44:137–143.
29. Lu H, Golay X, Pekar JJ, Van Zijl PC. Functional magnetic resonance imaging based on changes in vascular space occupancy. Magn Reson Med 2003;50:263–274.
30. Schwindt W, Burke M, Hoehn M. Activated areas found by BOLD, CBF, CBV and changes in CMRO2 during somatosensory stimulation do not co-localize in rat cortex. In: Proceedings of the Symposium on Brain Activation and CBF Control, International Congress Series 1235, Elsevier, 2002. p. 49–56.
31. Duong TQ, Kim D-S, Ugurbil K, Kim S-G. Localized cerebral blood flow response at submillimeter columnar resolution. Proc Natl Acad Sci USA 2001;98:10904–10909.